ORIGINAL ARTICLE

Disruption of RAB40AL function leads to Martin—Probst syndrome, a rare X-linked multisystem neurodevelopmental human disorder

Jirair Krikor Bedoyan,[1] Valerie M Schaibley,[2] Weiping Peng,[2] Yongsheng Bai,[3] Kajari Mondal,[4] Amol C Shetty,[4] Mark Durham,[1] Joseph A Micucci,[5] Arti Dhiraaj,[1] Jennifer M Skidmore,[1] Julie B Kaplan,[1] Cindy Skinner,[6] Charles E Schwartz,[6] Anthony Antonellis,[2] Michael E Zwick,[4] James D Cavalcoli,[3] Jun Z Li,[2,3] Donna M Martin[1,2]

ABSTRACT

Background and aim Martin—Probst syndrome (MPS) is a rare X-linked disorder characterised by deafness, cognitive impairment, short stature and distinct craniofacial dysmorphisms, among other features. The authors sought to identify the causative mutation for MPS.

Methods and results Massively parallel sequencing in two affected, related male subjects with MPS identified a *RAB40AL* (also called *RLGP*) missense mutation (chrX:102,079,078-102,079,079AC→GA p.D59G; hg18). *RAB40AL* encodes a small Ras-like GTPase protein with one suppressor of cytokine signalling box. The p.D59G variant is located in a highly conserved region of the GTPase domain between β-2 and β-3 strands. Using RT-PCR, the authors show that *RAB40AL* is expressed in human fetal and adult brain and kidney, and adult lung, heart, liver and skeletal muscle. *RAB40AL* appears to be a primate innovation, with no orthologues found in mouse, *Xenopus* or zebrafish. Western analysis and fluorescence microscopy of GFP-tagged RAB40AL constructs from transiently transfected COS7 cells show that the D59G missense change renders RAB40AL unstable and disrupts its cytoplasmic localisation.

Conclusions This is the first study to show that mutation of *RAB40AL* is associated with a human disorder. Identification of *RAB40AL* as the gene mutated in MPS allows for further investigations into the molecular mechanism(s) of RAB40AL and its roles in diverse processes such as cognition, hearing and skeletal development.

INTRODUCTION

Mutations in genes encoding Ras proteins are responsible for a number of human genetic disorders, including Costello (*HRAS*), Noonan (*KRAS* and *NRAS*), cardiofaciocutaneous (*KRAS*) and autoimmune lymphoproliferative (*NRAS*) syndromes.[1] [2] Ras proteins are components of the Ras/mitogen-activated protein kinase pathway and are important for proper cellular growth, differentiation and proliferation. Ras proteins canonically cycle (or switch) between active guanosine triphosphate (GTP)-bound and inactive guanosine

diphosphate (GDP)-bound conformations (Ras-GTP and Ras-GDP).[3] Ras proteins generate distinct signal outputs in cells, despite interacting with a common set of competing activators (GTPase activating proteins) and exchange factors (guanine nucleotide exchange factors) which regulate Ras-GTP levels.[4] [5] Ras proteins contain a hypervariable (HVR) domain within the C-terminal 25—50 amino acids. The HVR contains sites for post-translational lipid and other modifications and is the only region that differs significantly in sequence among the otherwise highly homologous Ras genes. HVR domains confer distinct biochemical properties of the Ras proteins and are involved in subcellular localisation and signal transduction. Cell- and tissue-specific expression may also contribute to the unique biological and developmental effects of Ras proteins.[6]

Rab GTPases belong to the Ras superfamily of small GTPases.[7] More than 50 Rab proteins have been described in mammalian cells, each with a specific subcellular localisation and many with specific patterns of tissue distribution.[8] [9] Rab proteins are involved in regulating intracellular vesicle transport and trafficking of proteins between organelles, behaving as membrane-associated molecular switches.[8] [9] The suppressor of cytokine signalling (SOCS) box distinguishes the four Rab40 proteins (Rab40a, Rab40al, Rab40b and Rab40c) from other Rab GTPases. SOCS box-containing proteins interact with an E3 ubiquitin ligase complex (with elongins B and C) that poly-ubiquitinates target proteins for subsequent degradation.[10] The target specificity of the complex is determined by a protein—protein interaction domain located N-terminal of the SOCS box-containing protein.[10] RAB40AL is a 278-amino acid Ras-like GTPase protein with a single SOCS box immediately proximal to the C-terminal HVR domain.

RAB40AL (*RLGP*) was previously implicated in a male person with an inversion (46,X,inv(X)(p21.2q22.2)) disrupting the *RAB40AL* promoter region.[11] This individual was diagnosed with congenital muscular dystrophy accompanied by severe intellectual disability, congenital nystagmus and athetosis. He never developed meaningful

speech nor sat without support, and died at 18 years of age from suffocation due to tracheal obstruction. He was also diagnosed with congenital Duchenne-type muscular dystrophy and harboured a deletion of *DMD* exons 43–60, but his severe intellectual disability was ascribed to the disruption of *RAB40AL* function.[11] The authors hypothesised that RAB40AL may play a critical role in the development or function of the central nervous system (CNS) by transducing signals or transporting molecules across mitochondrial membranes.[11]

Martin–Probst syndrome (MPS; MIM 300519) is a rare multi-organ system neurodevelopmental disorder initially charac-terised in three related male subjects with sensorineural hearing loss, cognitive impairment, short stature and craniofacial dysmorphisms.[12] MPS shares some characteristics with Costello syndrome (CS) and Noonan syndrome (NS) such as short stature, cognitive impairment and craniofacial dysmorphisms. However, unlike CS and NS, individuals with MPS also exhibit sensorineural hearing loss, renal insufficiency and impaired haematopoiesis.[12] [13] Additional clinical features seen in one individual with MPS (patient 1 in Martin *et al*,[12] same as indi-vidual II-1 in figure 1A) include chronic dyspnoea, pulmonary hypertension, septal cirrhosis and abnormal branching patterns of large hepatic vessels (unpublished data). The causative mutation for MPS was previously localised to a 68 megabase common haplotype region on X chromosome containing 683 genes between DXS1003 and DXS1220 (chrX:46,419,359-114,514,483; hg18; Xp11.3-Xq23).[12] [13] Deletions >1kb were excluded by PCR.[12] [13] Candidate genes *COL4A5*, *DIAPH2*, *POU3F4*, *ATRX*, *TIMM8A*, *XNP*, *ALEX2*, *KCNE1L* and *UBE1*, located within the 68 megabase target region, were previously excluded by direct sequencing or dHPLC.[12] [13] Female carriers in the pedigree have been found to exhibit non-random (or skewed) X-inactivation.[13] Here we provide evidence that a germline missense mutation in *RAB40AL* leads to MPS.

MATERIALS AND METHODS

DNA samples from individuals were obtained with informed consent as approved by the Institutional Review Board for Human Subject Research at the University of Michigan Medical Center.

Variant discovery and analysis via massively parallel sequencing

We performed whole genome sequencing (WGS), whole exome sequencing (WES) and X chromosome-specific exome[14] [15] sequencing to identify the causative mutation in MPS (see Supplemental Methods for detailed methods). It should be acknowledged that the word 'whole', used here in the context of massively parallel sequencing, does not imply absolute and complete coverage of all human genomic or exonic sequences.

Figure 1 *RAB40AL* p.D59G variant analysis and segregation. (A) The p.D59G variant identified in the sequenced individuals (III-5 and IV-1) segregates with the phenotype in the family. For individuals with a red dot, p.D59G was identified by Sanger sequencing. Affected individuals are shown in blue. For individuals with a green dot, p.D59G status was not determined. (B) Sequence chromatograms showing the two consecutive nucleotide changes (AC→GA) in a male subject (hemizygous) affected with MPS and an unaffected obligate female carrier (heterozygous). This change results in an Asp to Gly change at codon 59. Sanger sequencing readouts are shown. (C) The p.D59G variant (red) lies within a highly conserved 37 amino acid region of the GTPase domain and is conserved from humans to mosquitoes.
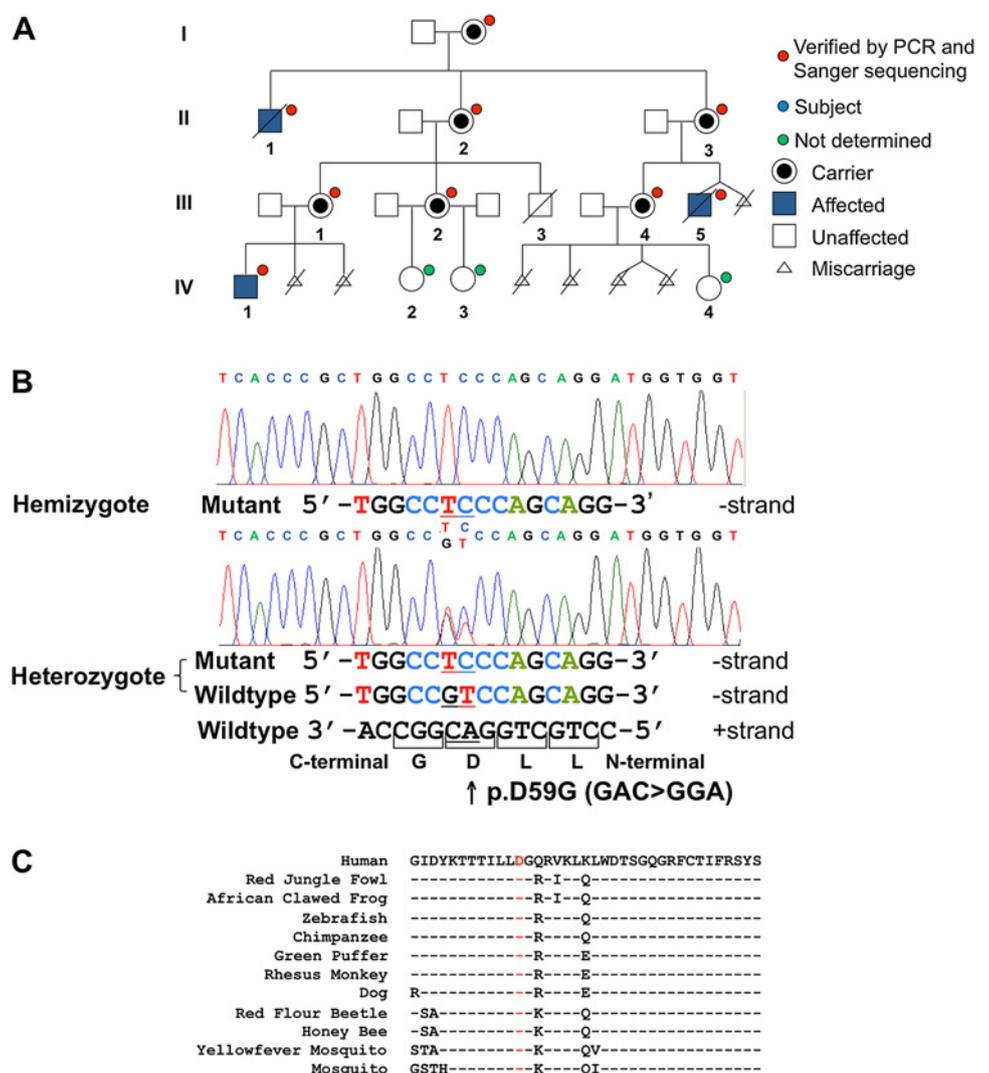
Coverage is limited by the repetitive nature and %GC content of the target genomic regions and by the actual probes used in the various exonic capture methods or reagents used. Reads from all three sequencing strategies were aligned to the reference human genome (UCSC hg18) using BWA.[16] For whole exome and whole genome data, SAMTools[17] was used to remove duplicate reads and call single nucleotide variants (SNVs) and indels. For X chromosome exome data, duplicate sequences were removed using PICARD and quality scores were recalibrated and variants called using GATK.[18] SNVs with a Phred quality score ≤30 or <4× coverage were excluded. SNVs were filtered through dbSNP130 and then imported into SeattleSeq for variant annotation. Variants were further filtered to exclude those identified by the 1000 Genomes Project (March 2010 release) or the National Heart, Lung, and Blood Institute Exome Sequencing Project. Predictions of functional effect of the missense variants were performed using PolyPhen,[19] PolyPhen-2,[19] MuPro,[20] SIFT[21] and AlignGVGD.[22 23] Measurements of the evolutionary conservation of the nucleotide were performed by GERP (from the original SeattleSeq annotation) and PhyloP. The Grantham matrix score was used to measure how different the two amino acids (wildtype vs mutant) are to each other.[24] Candidate genes with fetal nervous system expression (see the URL under Web resources) were verified by PCR/Sanger sequencing (data not shown).

Tissue expression

Clontech Multiple Tissue cDNA (Clontech, Mountain View, California, USA) panels from human fetal (Cat. #: 636747) and adult (Cat. #: 636742) tissues were used for expression analysis. Per Clontech certificate of analysis, the cDNA panels were generated from poly A+ RNA from the various tissues with assurance of original DNA contamination of <0.01% by pico green staining. Five μl (∼5 ng) of cDNA was mixed with 10 μl each (5 μM) of forward and reverse primers with 25 μl of 2× PCR Master mix (Cat. #: M7502; Promega, Madison, Wisconsin, USA). *RAB40AL* specific primers 5′ GCCTGCAGGACGG-CACGGCC 3′ and 5′ TCCCTCTTCCAGGTGTAACCATT 3′ were used along with human β-actin gene (*ACTB*) primers 5′ ATATCGCCGCGCTCGTCGTC 3′ and 5′ AGTGGTACGGC-CAGAGGCGT 3′. PCR conditions were 95°C for 2 min, followed by 30 cycles of 95°C for 30 s, 60°C for 1 min, 72°C for 1 min, and 72°C for 5 min. The PCR product was analysed by agarose gel electrophoresis.

GFP expression vector construction

pmCIT−C1 and pmCIT−N1 vectors (derivatives of Clontech pEGFP−C1 and −N1 vectors)[25] were used for generating expression constructs with RAB40AL tagged with green fluorescent protein (GFP). Standard molecular biology techniques were employed for engineering the constructs. The single exon *RAB40AL* was PCR amplified from human male control or patient DNA using primers 5′ <u>AGATCT</u>ATGAGCGCCCCGGG CAGCCCCGAC 3′ and 5′ <u>GTCGAC</u>TTAAGAAATTTTTGCAG CTGTTTCT 3′, or 5′ <u>CTCGAG</u>ATGAGCGCCCCGGGCAGCC CCGAC 3′ and 5′ <u>AAGCTT</u>AGAAATTTTTGCAGCTGTTTCT 3′ (restriction sites underlined). The first primer set engineers *Bgl*II and *Sal*I restriction sites at the 5′ and 3′ ends of the PCR product, respectively. These sites allow for inframe cloning of GFP and *RAB40AL* wild type or p.D59G variant coding sequence in pmCIT−C1 to generate N-terminal fusions. The second set of primers engineers *Xho*I and *Hind*III restriction sites at the 5′ and 3′ ends of the PCR products. These PCR products were cloned into pmCIT−N1 to generate C-terminal inframe

fusions of GFP to RAB40AL wild type or p.D59G variant. We used GFP−RAB40AL and GFP−RAB40AL−p.D59G to denote the N-terminal tagged constructs, and RAB40AL−GFP and RAB40AL−p.D59G−GFP to denote the C-terminal tagged constructs. Vector constructs were confirmed by Sanger sequencing for proper engineering and sequence accuracy.

Transfection and immunocytochemistry

COS7 cells were grown in DMEM with 10% FBS in a 12-well plate on round coverslips. At ∼90% confluence, transfection was performed with lipofectamine 2000 (Invitrogen, Carlsbad, California, USA). Specifically, 2 μg of vector DNA in water was diluted in 100 μl of Opti-MEM reduced serum media (GIBCO, Carlsbad, California, USA) for 5 min at room temperature. In addition, 5 μl of lipofectamine reagent was mixed with 100 μl of Opti-MEM reduced serum media and incubated for 5 min at room temperature. Both solutions were then combined and incubated for 20 min at room temperature. Subsequently, an additional 300 μl of Opti-MEM reduced serum media was added to the mix and the total volume then added to cells and incubated at 37°C for 4 h. Subsequently, 500 μl of DMEM with 10% FBS was added to the coverslips and cells incubated at 37°C for 48 h. Cells were then fixed with ice-cold methanol for 5 min, air dried, washed with PBS followed by two washes with PBS/Tween 20 (0.1%) 5 min each, and then treated with 1:500 dilution of mouse anti-human mitochondrial COXIV antibody (Cat. #: mAbcam33985; Abcam, Cambridge, Massachusetts, USA) and incubated overnight at 4°C. Following two more washes with PBS/Tween-20, Alexa Fluor 555 F(ab′)₂ fragment of goat antimouse IgG (Cat. #: A21425; Invitrogen) diluted 1:500 was added and incubated for 1 h at room temperature. Following two additional washes, cells were stained with DAPI (1:500 dilution in PBS), mounted and images captured on a Leica DM5000B microscope (W. Nuhsbaum Inc., McHenry, Illinois, USA). Transfection efficiencies were measured by determining the percentage of GFP+ cells among total DAPI+ cells transfected with vector only, WT construct or MUT construct. Nuclear clustering percentages were measured by determining the percentage of cells with fusion protein within the nucleus, nucleolus and/or perinuclear regions among all GFP+ cells.

Cell lysate preparation, PAGE and western analysis

Confluent COS7 cells in 12-well tissue culture plates were washed twice with ice-cold PBS and treated with 500 μl of RIPA buffer (Cat. #: R0278; Sigma, St. Louis, Missouri, USA) with 1% Protease Inhibitor Cocktail BD BaculoGold (Cat. #: 554779; BD Biosciences, San Diego, California, USA). After thoroughly mixing, the cell suspension was incubated on ice for 20 min with additional vortexing for complete lysis. The suspension was sonicated for 10 min and then centrifuged at 13 000 rpm for 5 min. The supernatant was collected and quantified using Bio-Rad Protein Assay kit (Cat. #: 500-0006; Bio-Rad, Hercules, California, USA). Approximately 30 μg of protein was added to 5 μl of NuPAGE sample buffer (Cat. #: NP0007; Invitrogen) along with 2 μl of NuPAGE reducing agent (Cat. #: NP0004; Invitrogen). The sample mix was heated for 10 min at 80°C. Precast Invitrogen NuPage 4−12% Bis-Tris gels (Cat. #: NP0322BOX; Invitrogen) were used for polyacrylamide gel electrophoresis (PAGE). NuPAGE antioxidant (0.25%) (NP0005; Invitrogen) was added to 200 ml of 1X MOPS (Cat. #: NP0001; Invitrogen) running buffer and poured in the centre of the apparatus. Untreated 1X MOPS was used in the remaining chamber. The gel was run at 200 V for 1.5 h and proteins transferred onto Immobilon PVDF transfer membranes

(IPSN07852; Millipore, Billerica, Massachusetts, USA) using NuPage Transfer buffer (Cat. #: NP0006-1; Invitrogen). Membranes were blocked overnight at 4°C with 5% BSA prepared in tris-buffered saline. Subsequently, the membranes were incubated for 2 h at room temperature with the primary mouse anti-GFP monoclonal antibody (Cat. #: 632380; Clontech) (or primary mouse anti-glyceraldehyde-3-phosphate dehydrogenase monoclonal antibody for detecting control house-keeping protein; Cat. #: MAB374, Millipore, Temecula, California, USA) followed by five washes (5 min each) with tris-buffered saline−0.5% Tween20. The membrane was then incubated with secondary anti-mouse horseradish peroxidase-conjugated antibody (Cat. #: 1858415; Pierce/Thermo Scientific, Rockford, Illinois, USA) for 1 h at room temperature. Washes were repeated and protein was detected using the chemiluminescence system (Cat. #: 34087; Thermo Scientific).

Statistical analysis of data

The SPSS Statistics program V.19 was used for statistical analysis of data. A general linear model was performed to examine: (1) transfection efficiencies (number of GFP+ cells/number of DAPI+ cells) among the three vectors and (2) the number of transfected cells with clustering of GFP fluorescence signal within the nucleus, nucleolus and/or perinuclear regions for the three vectors. Post hoc comparisons were performed to determine differences among the three groups with a Bonferroni correction.

RESULTS
RAB40AL is mutated in MPS

WGS, WES and X chromosome specific exome sequencing were performed to analyse DNA from two related male subjects affected with MPS (WGS, WES and X exome sequencing were performed for individual III-5, and X exome sequencing only was performed for individual IV-1; see table 1 and figure 1A). The average read depths per target region were 4.8 and 10.9X for WGS and WES, respectively, and 86.9X (for III-5) and 17.9X (for IV-1) for X-specific exome sequencing. Combining all three massively parallel sequencing strategies provided complete sequence coverage for 96.4% (3496/3625) of exons with ≥4× depth of coverage. Sixty-one of the remaining 129 exons were not covered by the three different sequencing strategies, yet were expressed in the fetal nervous system; the other 68 exons were not expressed in the human fetal nervous system and were excluded from further analysis. Forty-four of the remaining 61 exons were Sanger sequenced and revealed no potentially damaging or pathogenic variants (Supplemental table 1).

Seventeen exons proved difficult to sequence after multiple amplification attempts with different PCR primer pairs, presumably due to their high repetitive sequence nature and/or higher GC content.

Massively parallel sequencing analysis identified 15 candidate variants in 10 genes common to III-5 and IV-1 (table 1). Two genes, *RAB40AL* and *ARHGEF9*, contained missense mutations. Application of multiple protein function prediction algorithms showed the *RAB40AL* p.D59G variant (102,079,078-102,079,079AC→GA, hg18) to be highly damaging (table 1 and Supplemental table 2), while the *ARHGEF9* p.D306E variant (62,810,649G→C, hg18) was not considered damaging. *RAB40AL* was covered 100% with optimum coverage noted using the X-specific exome sequencing strategy (Supplemental figure 1).

The *RAB40AL* p.D59G variant segregated with the phenotype in MPS family members (figure 1A), and all obligate and non-obligate female subjects with X chromosome skewing were carriers of the mutation.[13] The AC→GA change in hemizygous male subjects and heterozygous female subjects and the resulting D59G amino acid substitution are shown in figure 1B. Asp59 (D59) is highly conserved from humans to mosquitoes (figure 1C). There were no p.D59G variants detected after: (a) direct sequencing of 297 neurologically normal control male subjects (250 of 297 were Caucasian) obtained from the Greenwood Genetic Center, National Institute of Neurological Disease and Coriell Institute for Medical Research and (b) analysis of the most recent 1000 Genomes Project dataset or the National Heart, Lung, and Blood Institute Exome Sequencing Project (∼3000 individuals of unknown gender; 10/2011 accessed). Based on published analytical approaches,[26] this number of controls provides >95% power to exclude *RAB40AL* p.D59G as a normal sequence variant with 0.1% frequency.

RAB40AL appears to be a primate innovation

In mammals, X chromosome genes maintain complete synteny because of the constraints imposed by X chromosome inactivation; however, some non-pseudoautosomal X chromosome genes violate this rule.[27] Detailed analysis of the corresponding syntenic region identified *RAB40AL* orthologues in primates such as rhesus monkeys and chimpanzees, but not in dog, rat, mouse, *Xenopus* or zebrafish (data not shown). Nucleotide- (using both 5′- and 3′-UTR regions as well as the complete gene) and protein-BLAST analyses of *RAB40AL* and RAB40AL, respectively, identified mouse Rab40b as the gene product with the highest identity (83%) and similarity (91%) to human RAB40AL; however, the orthologue of *Rab40b* on mouse chromosome 11 is

Table 1 Summary of whole genome, whole exome and X chromosome specific exome sequencing for two affected related individuals

	Individual III-5			Individual IV-1	
	Whole genome	**Whole exome**	**X exome**	**X exome**	**Shared variants**
Total variants	2 647 939	45 182	1718	1197	—
Novel variants	251 039	7869	300	192	—
Variants in haplotype block	3599	34	137	90	—
NS/MS/SS/UTR	27	9	25	18	15
Fetal nervous system expressed	—	—	—	—	7
Confirmed by sanger sequencing	—	—	—	—	2
Predicted damaging	—	—	—	—	1

The number of variants for each step in the analysis pipeline for the three distinct sequencing methods is shown. There were a total of 15 variants covering 12 genes shared among the two individuals (SSX4, FOXR2, RAB40AL, GRIPAP1, CLCN5, FOXR2, SPIN3, ARHGEF9, FAM123B, KIAA2022, AR, TRPC5). Of these 12 genes, seven were expressed in the fetal nervous system (GRIPAP1, CLCN5, SPIN3, ARHGEF9, FAM123B, KIAA2022, RAB40AL) and two of these genes (ARHGEF9 and RAB40AL) contained missense mutations and segregation with the phenotype in the family.
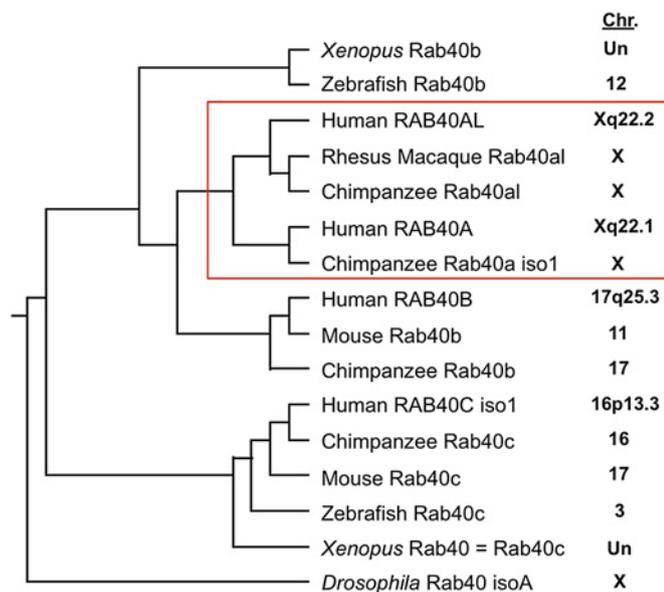MS, missense; NS, nonsense; SS, splice site; UTR, untranslated region.

Figure 2 Phylogenetic relationship of RAB40 family of proteins. Dendogram generated from protein sequences aligned using CLUSTAL W V.2.1 is shown. Synteny analyses of *RAB40AL* and *RAB40A* using UCSC Genome Browser did not identify mouse, *Xenopus* or zebrafish orthologues of human *RAB40AL*. The X-linked *RAB40AL* and *RAB40A* are unique to primates (red rectangle). Un, unknown.

Figure 3 *RAB40AL* expression in relevant fetal and adult human tissues. RT-PCR using Clontech multiple tissue cDNA panels from human fetal and adult tissues shows high *RAB40AL* expression in fetal and adult brain and kidney tissues, with lower levels of expression in fetal lung, heart, liver and skeletal muscle. Single bands corresponding to 812 bp and 437 bp for *RAB40AL* and β—*actin* PCR products, respectively, were observed as expected. Bands were also confirmed by Sanger sequencing. A, adult; F, fetal.

RAB40B on human chromosome 17 (figure 2; confirmed by synteny analysis). Human RAB40A shows 99% protein identity and similarity to RAB40AL; the *RAB40A* gene is ∼560 kb telomeric to *RAB40AL* on the X chromosome and is flanked by repetitive sequences. The phylogenetic relationship of the RAB40 family of proteins is shown in figure 2. The apparent restriction of *RAB40AL* to primates suggests a recent evolutionary divergence and is consistent with the hypothesised functional role of *RAB40AL* in neurodevelopment.

RAB40AL is expressed in fetal and adult human tissues including brain and kidney

Because individuals with MPS exhibit developmental delay and cognitive impairment, we hypothesised that *RAB40AL* should be expressed in both fetal and adult brain tissues. Analysis of RNA from fetal and adult human tissues using RT-PCR showed that *RAB40AL* is expressed in MPS-related tissues, including brain and kidney (figure 3), consistent with reported MPS phenotypes.[12] Based on this semiquantitative PCR-based expression analysis, *RAB40AL* expression levels in the fetal lung, heart, liver and skeletal muscle appeared lower than in adult tissues (figure 3), but this needs to be confirmed by quantitative methods. Others have also shown, by northern analysis, that *RAB40AL* is expressed in adult brain, heart, liver, skeletal muscle and kidney.[11]

The D59G missense change alters RAB40AL abundance in COS7 cells

Based on the location of D59 within the GTPase domain of RAB40AL, specifically within a conserved loop region located between two presumptive β-strands, we predicted that the D59G missense mutation might render it unstable, reducing function. The C-terminal HVR of RAB40AL contains sequence motifs that mediate attachment of lipid moieties predicted to anchor it to the phospholipid bilayer. Consequently, an unconstrained C-terminus may be critical for normal RAB40AL bio-
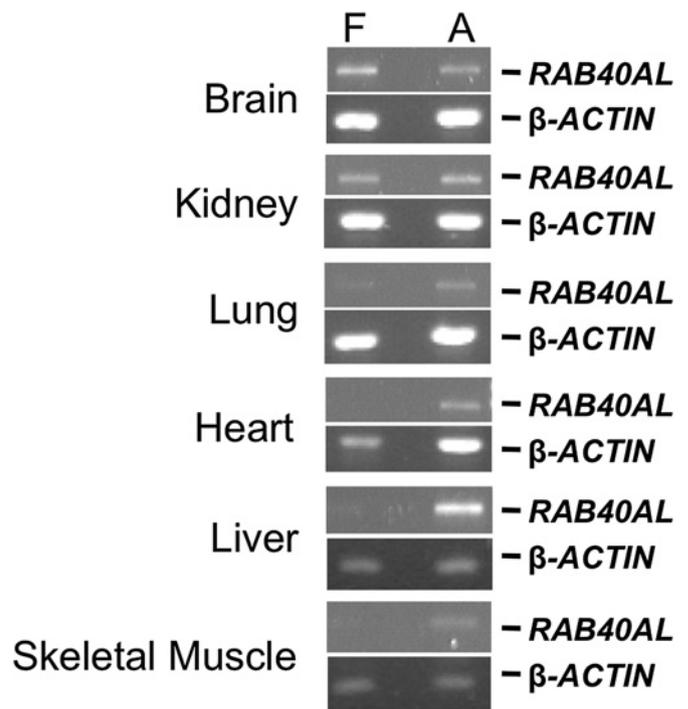
logical function. To test this, we constructed N-terminal and C-terminal GFP-tagged fusions of RAB40AL and RAB40AL—p.D59G and examined the impact of p.D59G by transient transfection and western analysis. Results of western analysis using anti-GFP monoclonal antibody of whole cell lysates from cells transiently transfected with these expression vectors are shown in figure 4. Both GFP (control vector alone) and WT GFP—RAB40AL were easily detected. In contrast, MUT GFP—RAB40AL—p.D59G fusion protein was significantly reduced compared with WT, despite similar transfection efficiencies (see table 2). We hypothesise that the reduced abundance of GFP—RAB40AL—p.D59G is due to instability and degradation of the fusion protein.

We observed low abundance bands from both RAB40AL—GFP and RAB40AL—p.D59G—GFP constructs, despite similar transfection efficiencies (data not shown). The low abundance of RAB40AL—GFP fusion protein suggests that constraining the RAB40AL C-terminus with a bulky (∼27 kDa GFP) protein disrupts RAB40AL function and renders it unstable. However, further analyses are needed to directly measure RAB40AL synthesis and degradation kinetics.

The D59G missense change disrupts RAB40AL cytoplasmic localisation

Previous studies have shown that RAB40AL localises to the mitochondria in COS7 cells.[11] In addition, analysis of the C-terminal 49 amino acid HVR of RAB40AL by MitoPred, a mitochondrial prediction algorithm, predicted mitochondrial localisation with 99% confidence (data not shown). This was not the case for *Xenopus* Rab40c or human RAB40C, where the
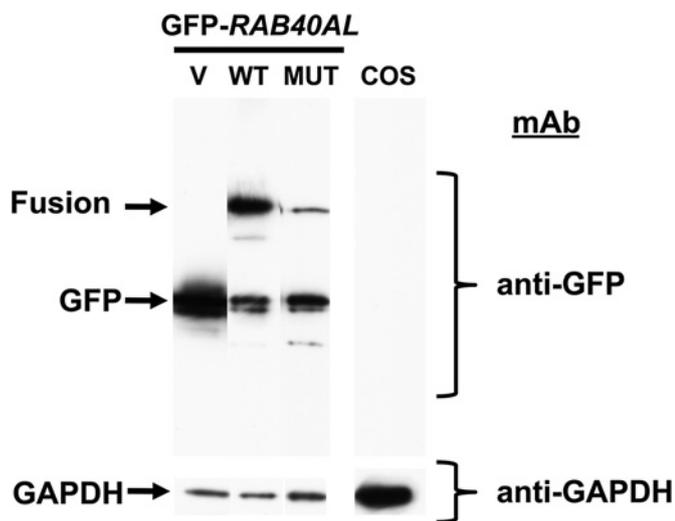
Figure 4 Reduced abundance of green fluorescent protein (GFP)—RAB40AL—p.D59G fusion protein in COS7 cells. Western analysis of whole cell lysates from cells transiently transfected with GFP—RAB40AL vector constructs (V, vector only; WT, GFP—RAB40AL; or MUT, GFP—RAB40AL p.D59G) using anti-GFP (or anti-GAPDH) monoclonal antibody (mAb). Results show reduced abundance of GFP—RAB40AL—p.D59G fusion protein, with essentially unchanged levels of the house-keeping GAPDH protein. Transfection efficiencies were not significantly different among the three vector constructs (see table 2). COS, untransfected COS7 cell lysate.

former is known to be localised to the Golgi.[28] Consequently, we examined whether the p.D59G variant disrupts this mitochondrial localisation (figure 5 and Supplemental figure 2). As expected, GFP—RAB40AL localised to the mitochondria but was also found diffusely throughout the cytoplasm (figure 5, panel H). This cytoplasmic localisation was disrupted in GFP—RAB40AL—p.D59G constructs and the fusion protein appeared to be accumulated or clustered within the nucleus, nucleolus and/or perinuclear region (figure 5, panels I and L). One-way ANOVA revealed that cells transfected with V, WT and MUT constructs were significantly different on 'nuclear clustering' efficiency ($F_{2,26} = 41.074$, p<0.001). Pairwise post hoc comparison indicated that cells transfected with the MUT construct (64.0±16.9; mean±SD) were significantly different than those transfected with WT (30.1±16.2; mean±SD) for per cent nuclear clustering (p<0.001) (see also table 2). Interestingly, the C-terminal GFP-tagged fusions (RAB40AL—GFP and RAB40AL—p.D59G—GFP) exhibited staining patterns similar to the N-terminal tagged mutant fusion construct (GFP—RAB40AL—p.D59G) (compare panels I and L in Supplemental figure 2 with panel L in figure 5). Thus, the D59G missense change appears to disrupt the normal localisation of RAB40AL, perhaps via mechanism that also render it prone to

degradation (figure 4). These data also suggest that the RAB40AL C-terminus is critical for protein stability and intracellular protein localisation.

DISCUSSION
We have identified a germline missense *RAB40AL* mutation (p.D59G) in individuals affected with MPS. This variant is predicted to be damaging using seven different DNA/protein functional inference algorithms, is absent in ∼3300 normal controls, segregates with the phenotype in the family and is located within a highly conserved GTPase region of the protein. *RAB40AL* is expressed in fetal and adult brain tissues, consistent with the cognitive impairments present in MPS individuals. Functional analysis of the p.D59G variant by transfection studies and western blotting showed that the variant renders the protein unstable and disrupts its normal cytoplasmic localisation. An unconstrained C-terminus appears necessary for normal RAB40AL localisation, based on transient transfections of N-terminal and C-terminal tagged wild type and mutant fusion constructs. We conclude that disruption of RAB40AL function by the p.D59G variant leads to MPS.

XLID, X-linked hearing loss and X-inactivation
MPS is one among approximately 200 X-linked intellectual disability (XLID) disorders.[29] The prevalence of XLID is approximately 1:1000 in male subjects, and XLID accounts for ∼16% of male subjects with intellectual disability.[29 30] Among the 1606 genes on the human X chromosome (Build 37.1), at least 87 have been identified as causative for XLID.[29 31 32] Several genes encoding GTP-binding proteins are reported to play critical roles in the development and function of the CNS, including several that participate in intracellular signalling or vesicular trafficking.[33–37] Data reported here support the hypothesis that RAB40AL is critical for normal development and function of CNS and *RAB40AL* can now be added to the list of syndromic XLID causative genes.

In addition to cognitive impairments, individuals with MPS have bilateral congenital sensorineural hearing loss.[12] X-linked forms of hearing loss account for ∼5% of all congenital hearing loss, and at least eight different causative genes have been described (*DFN1/TIMM8A, DFN2/PRPS1, DFN3/POU3F4, DFN6/SMPX, DFN7/GSTP1, NDP, FLNA* and *MED12*).[12 29] Mutations in *TIMM8A*, which encodes a mitochondrial intermembrane protein that interacts with a GTPase to regulate programmed cell death, causes Mohr—Tranebjaerg/deafness—dystonia syndrome.[38] Interestingly, several autosomal-linked small GTPase proteins, including the Rho GTPases, also contribute to hearing phenotypes.[39 40] To our knowledge, ours is the first study to show that mutation of *RAB40AL* is associated with hearing loss.

X-inactivation equalises the dosage between male and female subjects for most X chromosome genes, and this process is

Table 2 Quantitative analysis of transfection experiments

	V	WT	MUT	$F_{2,26}$	p Value
Transfection efficiency mean (SD)	42.1 (5.9)	44.7 (5.4)	41.1 (14.3)	0.434	0.653
Total DAPI cells counted	1530	1595	1841		
% Nuclear clustering mean (SD)	1.9 (2.1)	30.1 (16.2)	64.0 (16.9)	41.074	<0.001
Total GFP cells counted	627	692	715		
N	8	9	12		

ANOVA analysis was performed to determine the F and p values, and post hoc comparisons were performed to determine differences among the three groups with a Bonferroni correction (see text).
GFP, green fluorescent protein; MUT, GFP—RAB40AL—p.D59G; N, number of experiments; V, vector only; WT, GFP—RAB40AL SD, standard deviation.
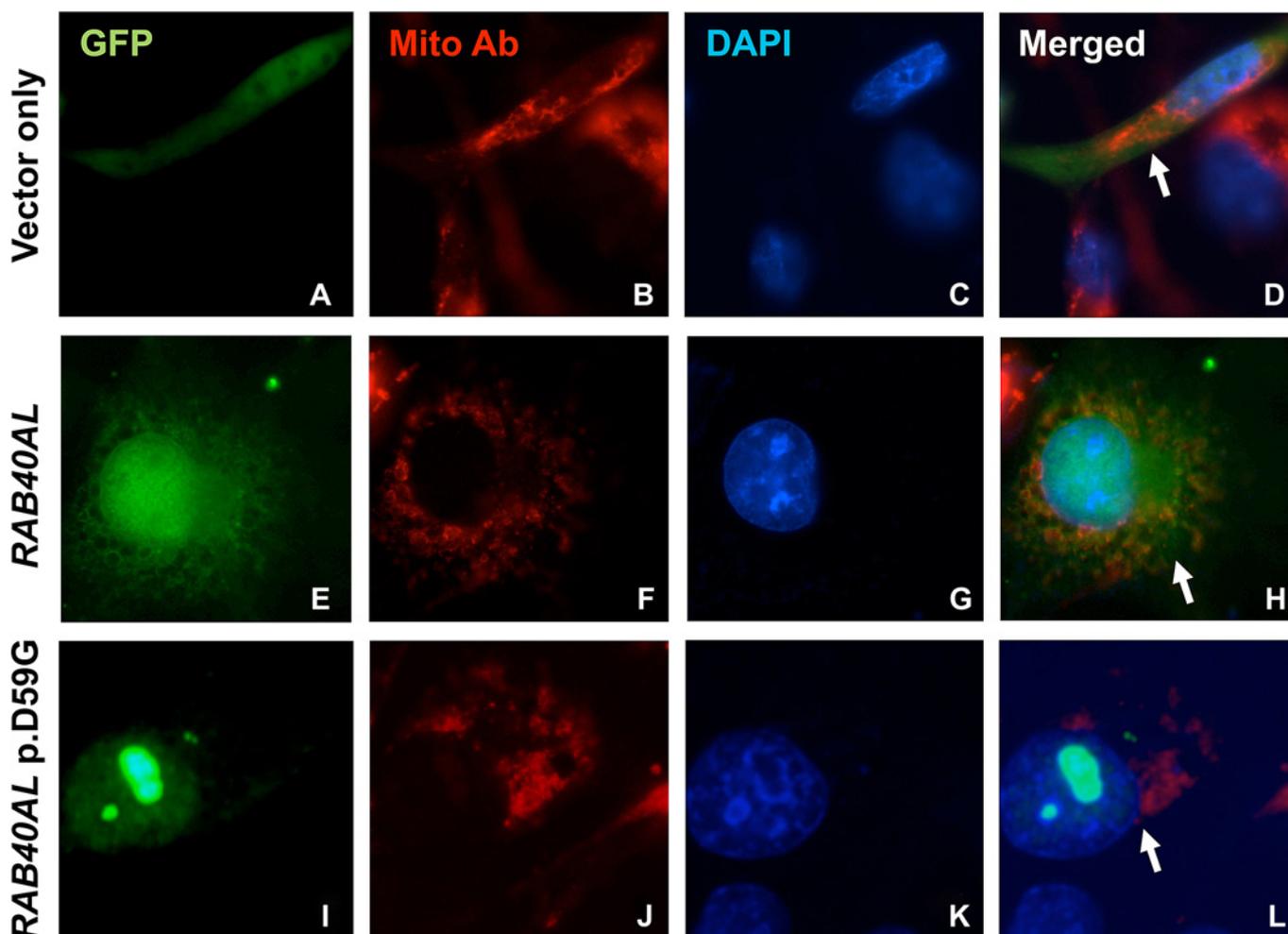
Figure 5 p.D59G disrupts normal intracellular protein localisation. Cells transiently transfected with N-terminal green fluorescent protein (GFP)-tagged vector constructs (vector control, A-D; *RAB40AL, E-H;* and *RAB40AL* p.D59G, I-L) and stained with anti-mitochondrial COXIV antibody (Mito Ab) and DAPI are shown. GFP–RAB40AL localises to the mitochondria and throughout the cytoplasm (panel H), while this localisation is disrupted with GFP–RAB40AL–p.D59G (panel L). GFP–RAB40AL–p.D59G appears to be accumulated or clustered within the nucleus, nucleolus and/or perinuclear region (panels I and L). Representative transfected cells are shown (arrows).

normally random in cells. In the presence of certain gene mutations and genomic alterations, the X chromosome bearing the altered gene or genomic region in female subjects is preferentially inactivated. Exceptions to this rule include cases where an X chromosome is translocated onto an autosome.[41] In MPS, four obligate and four non-obligate female heterozygous D59G mutation carriers show skewed X-inactivation and are clinically unaffected.[12 13] Interestingly, the unaffected mother of the male individual described by Saito-Ohara *et al* (2002)[11] was a carrier of the same inversion (46,X, inv(X)(p21.2q22.2)) but her X-inactivation status was not reported. Consequently, X chromosome inactivation skewing correlates with heterozygosity for the p.D59G variant and is another useful indicator of carrier status in MPS.

The RAB40AL p.D59G variant

Insights into the potential effect of D59G on RAB40AL function can be gained by examining the characteristics of the D47 aspartate residue (equivalent to RAB40AL D59) relevant for Rac other Ras-like proteins. D47 is predicted to be highly relevant for Rab function.[42] In addition to the known canonical function of GTPases of cycling between two states (ie, GDP vs GTP bound), phosphorylation of specific C-terminal serine residues in Ras

proteins is thought to act as an allosteric discriminator of conformational/dynamic states. Phosphorylation influences effector protein interactions with the GTPase protein at the switch loops/effector domain.[43] D47 in HRAS and RAP1B (another Ras-like protein) is located between the conserved β-2 and β-3 strands, and appears to be involved in facilitating this switch in conformational/dynamic states (from inactive to active) following S179 phosphorylation in the HVR domain.[43] Removal of D47 or E49 in HRAS negatively influences Ras signalling and orientation in the membrane.[44] The p.D59G variant may disrupt protein folding, nucleotide-binding (consequently, GTPase activity) or localisation rendering the protein non-functional and prone to degradation.

The Rab40 family

Current knowledge of the characteristics and roles of the various Rab40 proteins is limited. To date, the best characterised of the Rab40 proteins are the Rab40c family members. In *Xenopus, Rab40c* is required for normal gastrulation and embryogenesis.[28] Rab40c is localised at the Golgi apparatus and interacts with ElonginB/C and Cullin5 to form a ubiquitin ligase complex that selectively polyubiquitinates Rap2 and regulates non-canonical Wnt signalling.[28] In rat, *Rab40c* is expressed in oligodendrocytes

and is localised to the recycling endosomal compartment.[45] Human RAB40C is regulated directly by a cancer-related miRNA, *let-7a*, and mediates the biological effects of *let-7a* in gastric tumorigenesis.[46] Thus, Rab40c proteins have diverse functions in embryogenesis, ubiquitination and cancer.

In contrast to Rab40c, Rab40a and Rab40b function and intracellular localisation remain to be determined. *Rab40b* is expressed in the zebrafish brain (zebrafish database), suggesting a role in neurodevelopment. We found that mouse *Rab40b* is expressed in E14.5 embryonic and adult mouse brain, inner ear and heart tissues (data not shown). It remains to be determined, however, whether humans with mutated *RAB40B* also exhibit cognitive impairment and hearing loss, similar to individuals with MPS.

Unlike *RAB40C* and *RAB40B*, *RAB40A* and *RAB40AL* appear to be primate innovations (figure 3). A key approach for identifying orthologues of human genes in other species is synteny analysis, that is, exploiting the gene order conservation between species.[47 48] This approach identified orthologues of *RAB40AL* in primates only. Interestingly, primate specific genes display distinctive features including high tissue specificity, rapid evolution and short peptide size.[48] Some primate-specific genes are thought to have been formed by gene duplication,[48] and transposable elements also appear to play an important role.[48 49] Whether gene duplication or transposon-mediated events gave rise to *RAB40AL* in primates is not clear. There are at least several hundred genes that differ between human and mouse, most as a result of gene duplications or deletions.[50 51] The extent to which RAB40AL function overlaps with the other Rab40 members or is unique to primates is currently unknown. Study of the paralogue of *RAB40AL* (*Rab40b*) or introduction of human *RAB40AL* mutations into the mouse may provide insights into the roles of *RAB40B*, *RAB40A* and *RAB40AL* in brain, inner ear and other organ development.

SUMMARY

Using comprehensive variant discovery by high-throughput sequencing, we have identified *RAB40AL* p.D59G in the multi-organ system neurodevelopmental disorder MPS. The specific signalling pathway for RAB40AL and its particular mechanism and function in the mitochondria remain to be elucidated. Identification of *RAB40AL* mutations allows for detailed investigations into its molecular mechanism and functions in MPS, and should help improve diagnosis and treatment of individuals with related phenotypes.

REFERENCES

1. **Tidyman WE,** Rauen KA. The RASopathies: developmental syndromes of Ras/MAPK pathway dysregulation. *Curr Opin Genet Dev* 2009;**19**:230—6.
2. **Cirstea IC,** Kutsche K, Dvorsky R, Gremer L, Carta C, Horn D, Roberts AE, Lepri F, Merbitz-Zahradnik T, Konig R, Kratz CP, Pantaleoni F, Dentici ML, Joshi VA, Kucherlapati RS, Mazzanti L, Mundlos S, Patton MA, Silengo MC, Rossi C, Zampino G, Digilio C, Stuppia L, Seemanova E, Pennacchio LA, Gelb BD, Dallapiccola B, Wittinghofer A, Ahmadian MR, Tartaglia M, Zenker M. A restricted spectrum of NRAS mutations causes Noonan syndrome. *Nat Genet* 2010;**42**:27—9.
3. **Macaluso M,** Russo G, Cinti C, Bazan V, Gebbia N, Russo A. Ras family genes: an interesting link between cell cycle and cancer. *J Cell Physiol* 2002;**192**:125—30.
4. **Yan J,** Roy S, Apolloni A, Lane A, Hancock JF. Ras isoforms vary in their ability to activate Raf-1 and phosphoinositide 3-kinase. *J Biol Chem* 1998;**273**:24052—6.
5. **Voice JK,** Klemke RL, Le A, Jackson JH. Four human ras homologs differ in their abilities to activate Raf-1, induce transformation, and stimulate cell motility. *J Biol Chem* 1999;**274**:17164—70.
6. **Hancock JF.** Ras proteins: different signals from different locations. *Nat Rev Mol Cell Biol* 2003;**4**:373—84.
7. **Pereira-Leal JB,** Seabra MC. Evolution of the Rab family of small GTP-binding proteins. *J Mol Biol* 2001;**313**:889—901.
8. **Zerial M,** McBride H. Rab proteins as membrane organizers. *Nat Rev Mol Cell Biol* 2001;**2**:107—17.
9. **Stenmark H,** Olkkonen VM. The Rab GTPase family. *Genome Biol* 2001;**2**:3007.
10. **Kile BT,** Schulman BA, Alexander WS, Nicola NA, Martin HM, Hilton DJ. The SOCS box: a tale of destruction and degradation. *Trends Biochem Sci* 2002;**27**:235—41.
11. **Saito-Ohara F,** Fukuda Y, Ito M, Agarwala KL, Hayashi M, Matsuo M, Imoto I, Yamakawa K, Nakamura Y, Inazawa J. The Xq22 inversion breakpoint interrupted a novel Ras-like GTPase gene in a patient with Duchenne muscular dystrophy and profound mental retardation. *Am J Hum Genet* 2002;**71**:637—45.
12. **Martin DM,** Probst FJ, Camper SA, Petty EM. Characterisation and genetic mapping of a new X- linked deafness syndrome. *J Med Genet* 2000;**37**:836—41.
13. **Probst FJ,** Hedera P, Sclafani AM, Pomponi MG, Neri G, Tyson J, Douglas JA, Petty EM, Martin DM. Skewed X-inactivation in carriers establishes linkage in an X-linked deafness-mental retardation syndrome. *Am J Med Genet A* 2004;**131**:209—12.
14. **Patel VC,** Mondal K, Shetty AC, Horner VL, Bedoyan JK, Martin D, Caspary T, Cutler DJ, Zwick ME. Microarray oligonucleotide probe designer (MOPeD): a web service. *Open Access Bioinformatics* 2010;**2**:145—55.
15. **Okou DT,** Locke AE, Steinberg KM, Hagen K, Athri P, Shetty AC, Patel V, Zwick ME. Combining microarray-based genomic selection (MGS) with the illumina genome analyzer platform to sequence diploid target regions. *Ann Hum Genet* 2009;**73**:502—13.
16. **Li H,** Durbin R. Fast and accurate short read alignment with burrows-wheeler transform. *Bioinformatics* 2009;**25**:1754—60.
17. **Li H,** Handsaker B, Wysoker A, Fennell T, Ruan J, Homer N, Marth G, Abecasis G, Durbin R. The sequence alignment/map format and SAMtools. *Bioinformatics* 2009;**25**:2078—9.
18. **McKenna A,** Hanna M, Banks E, Sivachenko A, Cibulskis K, Kernytsky A, Garimella K, Altshuler D, Gabriel S, Daly M, DePristo MA. The genome analysis toolkit: a mapreduce framework for analyzing next-generation DNA sequencing data. *Genome Res* 2010;**20**:1297—303.
19. **Adzhubei IA,** Schmidt S, Peshkin L, Ramensky VE, Gerasimova A, Bork P, Kondrashov AS, Sunyaev SR. A method and server for predicting damaging missense mutations. *Nat Methods* 2010;**7**:248—9.

Web resources

The URLs for data presented are as follows:
- AlignGVGD; http://agvgd.iarc.fr/agvgd_input.php
- CLUSTAL W version 2.1; http://www.genome.jp/tools/clustalw/
- Human fetal nervous system expression database; http://bgee.unil.ch/bgee/
- MitoPred, http://bioapps.rit.albany.edu/MITOPRED/
- MuPro; http://mupro.proteomics.ics.uci.edu/
- NHLBI Exome Sequencing Project (Exome Variant Server); http://snp.gs.washington.edu/EVS/
- PhyloP; http://genome.ucsc.edu/
- PICARD; http://picard.sourceforge.net/
- PolyPhen; http://genetics.bwh.harvard.edu/pph/
- PolyPhen-2; http://genetics.bwh.harvard.edu/pph2/
- SeattleSeq; http://gvs.gs.washington.edu/SeattleSeqAnnotation/index.jsp
- SIFT; http://sift.jcvi.org/
- UCSC Genome Browser; http://genome.ucsc.edu
- Zebrafish database; http://zfin.org

20. **Cheng J,** Randall A, Baldi P. Prediction of protein stability changes for single-site mutations using support vector machines. *Proteins* 2006;**62**:1125—32.
21. **Kumar P,** Henikoff S, Ng PC. Predicting the effects of coding non-synonymous variants on protein function using the SIFT algorithm. *Nat Protoc* 2009;**4**:1073—81.
22. **Tavtigian SV,** Deffenbaugh AM, Yin L, Judkins T, Scholl T, Samollow PB, de Silva D, Zharkikh A, Thomas A. Comprehensive statistical study of 452 BRCA1 missense substitutions with classification of eight recurrent substitutions as neutral. *J Med Genet* 2006;**43**:295—305.
23. **Mathe E,** Olivier M, Kato S, Ishioka C, Hainaut P, Tavtigian SV. Computational approaches for predicting the biological effect of p53 missense mutations: a comparison of three sequence analysis based methods. *Nucleic Acids Res* 2006;**34**:1317—25.
24. **Grantham R.** Amino acid difference formula to help explain protein evolution. *Science* 1974;**185**:862—4.
25. **Rizzo MA,** Springer GH, Granada B, Piston DW. An improved cyan fluorescent protein variant useful for FRET. *Nat Biotechnol* 2004;**22**:445—9.
26. **Collins JS,** Schwartz CE. Detecting polymorphisms and mutations in candidate genes. *Am J Hum Genet* 2002;**71**:1251—2.
27. **Palmer S,** Perry J, Ashworth A. A contravention of Ohno's law in mice. *Nat Genet* 1995;**10**:472—6.
28. **Lee RH,** Iioka H, Ohashi M, Iemura S, Natsume T, Kinoshita N. XRab40 and XCullin5 form a ubiquitin ligase complex essential for the noncanonical Wnt pathway. *EMBO J* 2007;**26**:3592—606.
29. **Stevenson RE,** Schwartz CE. X-linked intellectual disability: unique vulnerability of the male genome. *Dev Disabil Res Rev* 2009;**15**:361—8.
30. **Chiurazzi P,** Schwartz CE, Gecz J, Neri G. XLMR genes: update 2007. *Eur J Hum Genet* 2008;**16**:422—34.
31. **Tarpey PS,** Smith R, Pleasance E, Whibley A, Edkins S, Hardy C, O'Meara S, Latimer C, Dicks E, Menzies A, Stephens P, Blow M, Greenman C, Xue Y, Tyler-Smith C, Thompson D, Gray K, Andrews J, Barthorpe S, Buck G, Cole J, Dunmore R, Jones D, Maddison M, Mironenko T, Turner R, Turrell K, Varian J, West S, Widaa S, Wray P, Teague J, Butler A, Jenkinson A, Jia M, Richardson D, Shepherd R, Wooster R, Tejada MI, Martinez F, Carvill G, Goliath R, de Brouwer AP, van Bokhoven H, Van Esch H, Chelly J, Raynaud M, Ropers HH, Abidi FE, Srivastava AK, Cox J, Luo Y, Mallya U, Moon J, Parnau J, Mohammed S, Tolmie JL, Shoubridge C, Corbett M, Gardner A, Haan E, Rujirabanjerd S, Shaw M, Vandeleur L, Fullston T, Easton DF, Boyle J, Partington M, Hackett A, Field M, Skinner C, Stevenson RE, Bobrow M, Turner G, Schwartz CE, Gecz J, Raymond FL, Futreal PA, Stratton MR. A systematic, large-scale resequencing screen of X-chromosome coding exons in mental retardation. *Nat Genet* 2009;**41**:535—43.
32. **Lisik MZ,** Sieron AL. X-linked mental retardation. *Med Sci Monit* 2008;**14**:RA221—9.
33. **Nakano-Kobayashi A,** Kasri NN, Newey SE, Van Aelst L. The rho-linked mental retardation protein OPHN1 controls synaptic vesicle endocytosis via endophilin A1. *Curr Biol* 2009;**19**:1133—9.
34. **Oh D,** Han S, Seo J, Lee JR, Choi J, Groffen J, Kim K, Cho YS, Choi HS, Shin H, Woo J, Won H, Park SK, Kim SY, Jo J, Whitcomb DJ, Cho K, Kim H, Bae YC, Heisterkamp N, Choi SY, Kim E. Regulation of synaptic Rac1 activity, long-term potentiation maintenance, and learning and memory by BCR and ABR Rac GTPase-activating proteins. *J Neurosci* 2010;**30**:14134—44.
35. **Bergmann C,** Zerres K, Senderek J, Rudnik-Schoneborn S, Eggermann T, Hausler M, Mull M, Ramaekers VT. Oligophrenin 1 (OPHN1) gene mutation causes syndromic X-linked mental retardation with epilepsy, rostral ventricular enlargement and cerebellar hypoplasia. *Brain* 2003;**126**:1537—44.
36. **Sakane A,** Miyoshi J, Takai Y, Sasaki T. Analysis on the emerging role of Rab3 GTPase-activating protein in Warburg Micro and Martsolf syndrome. *Methods Enzymol* 2008;**438**:131—9.
37. **Shimojima K,** Sugawara M, Shichiji M, Mukaida S, Takayama R, Imai K, Yamamoto T. Loss-of-function mutation of collybistin is responsible for X-linked mental retardation associated with epilepsy. *J Hum Genet* 2011;**56**:561—5.
38. **Arnoult D,** Rismanchi N, Grodet A, Roberts RG, Seeburg DP, Estaquier J, Sheng M, Blackstone C. Bax/Bak-dependent release of DDP/TIMM8a promotes Drp1-mediated mitochondrial fission and mitoptosis during programmed cell death. *Curr Biol* 2005;**15**:2112—18.
39. **Kollmar R.** Who does the hair cell's do? Rho GTPases and hair-bundle morphogenesis. *Curr Opin Neurobiol* 1999;**9**:394—8.
40. **Heidrych P,** Zimmermann U, Bress A, Pusch CM, Ruth P, Pfister M, Knipper M, Blin N. Rab8b GTPase, a protein transport regulator, is an interacting partner of otoferlin, defective in a human autosomal recessive deafness form. *Hum Mol Genet* 2008;**17**:3814—21.
41. **Yang C,** Chapman AG, Kelsey AD, Minks J, Cotton AM, Brown CJ. X-chromosome inactivation: molecular mechanisms from the human perspective. *Hum Genet* 2011;**130**:175—85.
42. **Heo WD,** Meyer T. Switch-of-function mutants based on morphology classification of Ras superfamily small GTPases. *Cell* 2003;**113**:315—28.
43. **Edreira MM,** Li S, Hochbaum D, Wong S, Gorfe AA, Ribeiro-Neto F, Woods VL Jr, Altschuler DL. Phosphorylation-induced conformational changes in Rap1b: allosteric effects on switch domains and effector loop. *J Biol Chem* 2009;**284**:27480—6.
44. **Abankwa D,** Hanzal-Bayer M, Ariotti N, Plowman SJ, Gorfe AA, Parton RG, McCammon JA, Hancock JF. A novel switch region regulates H-ras membrane orientation and signal output. *EMBO J* 2008;**27**:727—35.
45. **Rodriguez-Gabin AG,** Almazan G, Larocca JN. Vesicle transport in oligodendrocytes: probable role of Rab40c protein. *J Neurosci Res* 2004;**76**:758—70.
46. **Yang Q,** Jie Z, Cao H, Greenlee AR, Yang C, Zou F, Jiang Y. Low-level expression of let-7a in gastric cancer and its involvement in tumorigenesis by targeting RAB40C. *Carcinogenesis* 2011;**32**:713—22.
47. **Knowles DG,** McLysaght A. Recent de novo origin of human protein-coding genes. *Genome Res* 2009;**19**:1752—9.
48. **Toll-Riera M,** Bosch N, Bellora N, Castelo R, Armengol L, Estivill X, Mar Alba M. Origin of primate orphan genes: a comprarative genomics approach. *Mol Biol Evol* 2009;**26**:603—12.
49. **Toll-Riera M,** Castelo R, Bellora N, Alba MM. Evolution of primate orphan genes. *Biochem Soc Trans* 2009;**37**:778—82.
50. **Church DM,** Goodstadt L, Hillier LW, Zody MC, Goldstein S, She X, Bult CJ, Agarwala R, Cherry JL, DiCuccio M, Hlavina W, Kapustin Y, Meric P, Maglott D, Birtle Z, Marques AC, Graves T, Zhou S, Teague B, Potamousis K, Churas C, Place M, Herschleb J, Runnheim R, Forrest D, Amos-Landgraf J, Schwartz DC, Cheng Z, Lindblad-Toh K, Eichler EE, Ponting CP. Lineage-specific biology revealed by a finished genome assembly of the mouse. *PLoS Biol* 2009;**7**:e1000112.
51. **Waterston RH,** Lindblad-Toh K, Birney E, Rogers J, Abril JF, Agarwal P, Agarwala R, Ainscough R, Alexandersson M, An P, Antonarakis SE, Attwood J, Baertsch R, Bailey J, Barlow K, Beck S, Berry E, Birren B, Bloom T, Bork P, Botcherby M, Bray N, Brent MR, Brown DG, Brown SD, Bult C, Burton J, Butler J, Campbell RD, Carninci P, Cawley S, Chiaromonte F, Chinwalla AT, Church DM, Clamp M, Clee C, Collins FS, Cook LL, Copley RR, Coulson A, Couronne O, Cuff J, Curwen V, Cutts T, Daly M, David R, Davies J, Delehaunty KD, Deri J, Dermitzakis ET, Dewey C, Dickens NJ, Diekhans M, Dodge S, Dubchak I, Dunn DM, Eddy SR, Elnitski L, Emes RD, Eswara P, Eyras E, Felsenfeld A, Fewell GA, Flicek P, Foley K, Frankel WN, Fulton LA, Fulton RS, Furey TS, Gage D, Gibbs RA, Glusman G, Gnerre S, Goldman N, Goodstadt L, Grafham D, Graves TA, Green ED, Gregory S, Guigo R, Guyer M, Hardison RC, Haussler D, Hayashizaki Y, Hillier LW, Hinrichs A, Hlavina W, Holzer T, Hsu F, Hua A, Hubbard T, Hunt A, Jackson I, Jaffe DB, Johnson LS, Jones M, Jones TA, Joy A, Kamal M, Karlsson EK, Karolchik D, Kasprzyk A, Kawai J, Keibler E, Kells C, Kent WJ, Kirby A, Kolbe DL, Korf I, Kucherlapati RS, Kulbokas EJ, Kulp D, Landers T, Leger JP, Leonard S, Letunic I, Levine R, Li J, Li M, Lloyd C, Lucas S, Ma B, Maglott DR, Mardis ER, Matthews L, Mauceli E, Mayer JH, McCarthy M, McCombie WR, McLaren S, McLay K, McPherson JD, Meldrim J, Meredith B, Mesirov JP, Miller W, Miner TL, Mongin E, Montgomery KT, Morgan M, Mott R, Mullikin JC, Muzny DM, Nash WE, Nelson JO, Nhan MN, Nicol R, Ning Z, Nusbaum C, O'Connor MJ, Okazaki Y, Oliver K, Overton-Larty E, Pachter L, Parra G, Pepin KH, Peterson J, Pevzner P, Plumb R, Pohl CS, Poliakov A, Ponce TC, Ponting CP, Potter S, Quail M, Reymond A, Roe BA, Roskin KM, Rubin EM, Rust AG, Santos R, Sapojnikov V, Schultz B, Schultz J, Schwartz MS, Schwartz S, Scott C, Seaman S, Searle S, Sharpe T, Sheridan A, Shownkeen R, Sims S, Singer JB, Slater G, Smit A, Smith DR, Spencer B, Stabenau A, Stange-Thomann N, Sugnet C, Suyama M, Tesler G, Thompson J, Torrents D, Trevaskis E, Tromp J, Ucla C, Ureta-Vidal A, Vinson JP, Von Niederhausern AC, Wade CM, Wall M, Weber RJ, Weiss RB, Wendl MC, West AP, Wetterstrand K, Wheeler R, Whelan S, Wierzbowski J, Willey D, Williams S, Wilson RK, Winter E, Worley KC, Wyman D, Yang S, Yang SP, Zdobnov EM, Zody MC, Lander ES. Initial sequencing and comparative analysis of the mouse genome. *Nature* 2002;**420**:520—62.